Truth Cube: Establishing Physical Standards for Real Time Soft Tissue Simulation

Amy E. Kerdok[1], Stephane M. Cotin[2], Mark P. Ottensmeyer[2], Anna Galea[1], Robert D. Howe[1], Steven L. Dawson[2]

[1] Division of Engineering and Applied Sciences, Harvard University
[2] CIMIT Simulation Group, Massachusetts General Hospital
kerdok@fas.harvard.edu, 29 Oxford St. Pierce Hall, Cambridge, MA 02138, USA
phone 617.496.9098, fax 617.495.9837, http://biorobotics.harvard.edu

Keywords: soft tissue modeling, medical simulation, real-time, finite element modeling, validation

Abstract

Accurate and real-time models of soft tissue behavior are key elements in the development of medical simulation systems. However, precise validation of these models remains a challenge. Currently, real-time modeling is at best validated against FEM models that have their own intrinsic limitations. This study is the first in a series that will develop physical standards resulting in a database of relevant information used to validate real-time soft tissue deformation. In this first study, a simple 8cm cube of silicone rubber with an exact pattern of embedded Teflon beads was tested in uniaxial compression while CT images were taken. The known material properties, geometry, and carefully controlled boundary conditions resulted in a complete set of volumetric displacement data. The results were also compared to an FEM analysis of an identical situation. This work has served as a proof of concept for a robust physical standard for use in validating real-time models. A web site has been created to provide access to our database at:
http://biorobotics.harvard.edu/truthcube/.

1. Introduction

Fast, realistic mechanical modeling of soft tissues remains a formidable challenge in the development of new medical applications. Medical training, surgical planning, and image-guidance systems require real-time calculation of tissue shape and interaction forces as the user manipulates the simulated tissue.

Implementation of these modeling systems has proved difficult. The most frequently used approaches to simulating tissue deformation in real-time have been spring-mass models and, more recently, finite element methods (FEM). This has proved relatively unsatisfactory: surgical applications involve large deformations of nonlinear soft materials and require very rapid calculations. Spring-mass systems have limited accuracy but work in real-time, while FEM has proved successful for modeling small deformations of linear engineering materials where calculation speed is not a paramount concern. Many schemes have been proposed to overcome these limitations [e.g. Pic01, De01, Ast98, Kuh97, and Cot96], often balancing execution speed and mechanical accuracy. The nature of this tradeoff is not well understood, and it is difficult to evaluate the relative performance of new systems when speed, accuracy, tissue properties, and geometry all vary.

Progress towards effective real-time simulation would be aided by a consistent means of evaluating tissue mechanics models. Ideally, this evaluation method would provide a “gold standard” of experimental results for comparison with simulation results. This would take the form of fully specified material properties and stress, strain, and displacement fields throughout the tissue, under a range of fully specified and surgically relevant boundary conditions. The output of new modeling systems could then be compared to these standard results to validate and benchmark their performance.

We are working to create such a database of experimental measurements. The goal is to incorporate measurements for rubber phantoms with simple geometry and for a range of more complex materials including biological tissues and organs. These results will be archived on a web site for widespread access. This paper reports our initial effort, on the deformation of a cube of soft polymer. This 8 cm “truth cube” is made of a well-characterized silicone rubber with fiducials embedded in a 1 cm grid pattern throughout its volume. We have acquired computer tomography (CT) scans of the cube in undeformed and loaded states, and extracted the displacement of each fiducial using image processing techniques. Here we report these displacement results, along with details of the cube construction and boundary conditions in the loading tests. We conclude with a discussion of plans for extension of this work, and an invitation for participation by others interested in the validation of fast large-deformation tissue modeling.

2. Methods

We have selected a cube as a simple, regular shape for this initial effort to assess the feasibility of the approach and develop the required techniques. The considerations include the materials of the "tissue" and fiducials, 3-D imaging, image processing, and data reporting.

2.1 Truth Cube

We selected a 2-part silicone rubber (RTV6166, General Electric Co.) because of its proven success in simulating tissues [Ott00, Wel99]. The material is soft but exhibits linear behavior to at least 30% strain. To enable tracking of the internal displacements of the cube we embedded small beads as fiducials that would readily appear in CT scans but not significantly alter the material properties of the silicone. The choice of bead material and size was motivated both by the need for high contrast without creating imaging artifacts [Str98]; this implies a specific gravity well above silicone (0.98) but much less than steel (~8). To enable accurate segmentation and position estimation, the minimum diameter of the beads had to be slightly larger than the distance between two successive scanning planes (1.25 mm) but small enough to avoid compromising the material properties of the silicone. Imaging tests revealed that Teflon beads (specific gravity 2.3) with a diameter of 1.58 mm fulfilled all of these criteria.

The mold for the cube had removable sides, with the bottom serving as a rigid permanent mounting plate and was roughened and dimpled to ensure complete adhesion of the silicone. The two-part silicone rubber was mixed in a 30:70 proportion to obtain material characteristics similar to that of soft tissue. A layer 1 cm deep was poured, the mold was placed in a vacuum chamber to remove air bubbles, and then allowed to set on a leveled surface (~3.5 hours) before positioning the beads in a 7 x 7 matrix spaced 1 cm apart (Figure 1). The beads were laid on the rubber using a matrix of bead positioning tubes and allowed to set into the rubber for at least another hour before the next layer was poured. The end result produced an $8cm^3$ silicone rubber cube with 7 rows and 7 columns of Teflon® beads in 7 layers spaced 1cm apart (Figure 2).

To ensure that the material properties of the silicone rubber were not affected by the addition of the 343 beads, we performed indentation tests on a sample of the silicone rubber alone, on a sample with sparse bead density, and on a sample with 1 cm bead spacing. Results indicated that the stiffness of the sample with the highest bead density (780 N/m) changed 2%, less than the 4.4% standard deviation of measurements of the plain sample. We thus assume that the addition of the beads had a negligible effect on the material properties of the silicone.

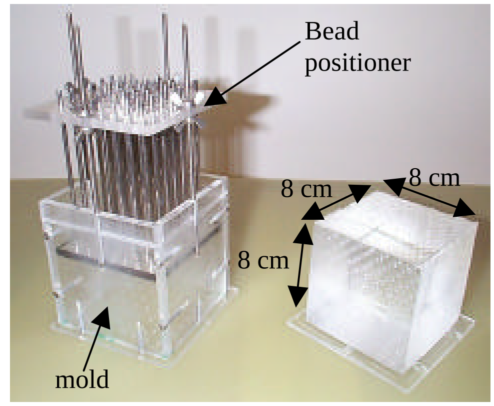

Figure 1: (left) Mold and bead positioner and (right) resulting "Truth Cube"

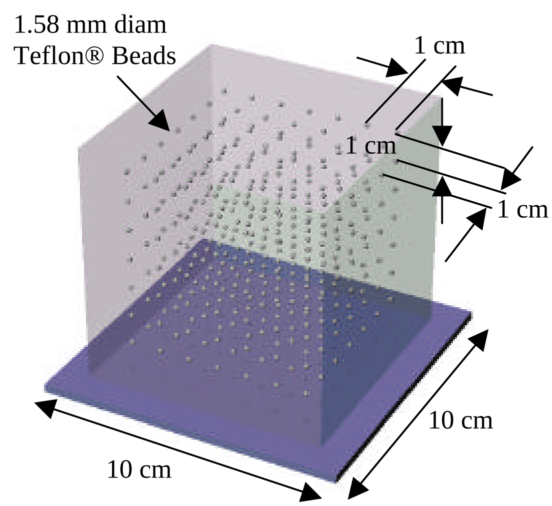

Figure 2: Dimensional drawing of "Truth Cube"

Both a small strain (<8%) uniaxial compression test and an indentation test were performed on a sample of the rubber used to obtain material property characteristics. Results indicate a Young's modulus of 14.9 ± 1.4 kPa. We assume that Poisson's ratio is near 0.5 for this polymer; volumetric data from the loaded state below showed minor compression, but this difference was less than the measurement accuracy.

2.2 Experimental Set-up

The test set-up for loading the cube must apply carefully controlled boundary conditions during the CT imaging process. The fixture base was constructed of 25.4 mm thick PVC (specific gravity 1.37) to span the width of the scan table for support (Figure 3). A pocket that tightly fit the rubber cube's base plate was cut into the fixture base. To ensure accurate positioning of the cube each time it was tested, various reference features were incorporated into the test fixture. The fixture base also included registration markers consisting of machined holes and grooves in "X" patterns, and Delrin spheres (specific gravity 1.4) positioned at the cube base corners and on top of a central post (visible in Figure 4A, B).

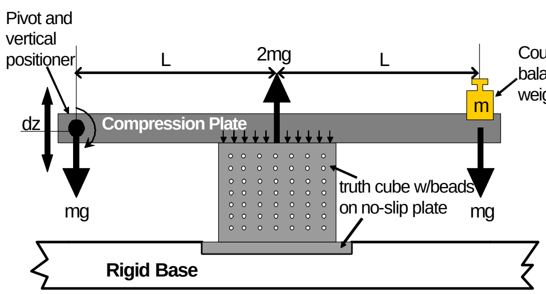

Figure 3: Side view of the experimental set-up. L is the length from the loading points to the center of the cube, dz is the vertical motion, and m is the mass of the counter weights.

The initial loading test reported here, uniaxial compression, was accomplished with a 25.4 mm thick acrylic plate (specific gravity 1.17). This was attached by a low-friction pivot to a vertical support. The plate was loaded by metal weights applied to the end opposite the pivot (in addition to the weight of the plate itself). The design confined all metal parts (the vertical support rods and weights) to the ends of the apparatus, so that they did not interfere with CT scanning of the cube in the middle of the apparatus. A linear dial indicator measured the distance the plate was compressed.

2.3 Experimental Protocol

A first scan of the experimental setup was performed while the cube was unloaded. The flat compression plate was then held level as it was lowered onto the oiled top surface of the cube to a set displacement. With the pivot end of the compression plate held in place, masses were added to a pocket in the other end until equilibrium was established as determined by level indicators. Three loading conditions were scanned: 4 mm, 10 mm, and 14.6 mm displacements producing 5.0%, 12.5%, and 18.25% nominal strain respectively.

Once loaded, the cube was scanned in a General Electric LightSpeed CT scanner. Volumetric images of the "truth cube" were then obtained using the following scanner settings: 120kV, 180mA, standard reconstruction type, and high quality scan mode. The field of view was of 190 mm, producing a voxel size of 0.37109 x 0.37109 x 1.25 mm^3. Each CT scan was composed of 99 slices (512 x 512 pixels, 16 bits) exported in DICOM format.

2.4 Image Processing

Commercial software (3D-Doctor, Able Software Corp., Lexington, MA) was used for manipulating the volumetric images. First, the minor artifacts present in the lower part of the cube (due to the PVC support plate) were filtered. Second, fiducial beads in each of the scans were segmented from the gel with thresholding; this was straightforward due to the relatively good contrast between the beads and the silicone gel, and all 343 beads were readily extracted. Surface models were then calculated in a format suitable for further processing.

The beads in the silicone cube have a size close to the size of a voxel, so the three-dimensional segmentation process only provided an approximation of the shape and location of the beads. To further analyze the data it was necessary to accurately determine the location of the center of each bead. We implemented a least squares algorithm that fit a sphere to the set of points defined by the vertices of the segmented beads. This algorithm is part of visualization software that visually assesses the quality of the fit, saves the information to files, and displays polygonal models and vector fields.

Computation of the displacement vectors of the beads between various loading conditions required the solution of a relatively complex matching problem. We therefore used a manual matching approach for this first set of experiments. Finally, the outermost three-dimensional surfaces of the cube at each compression stage were extracted from the images. Registration marks were also segmented in order to evaluate potential motion of the experimental setup between successive scans.

2.5 Finite Element Model Comparison

A finite element model of the truth cube using commercial FEM software (ABAQUS v. 5.8, Hibbitt, Karlsson & Sorensen, Inc., Pawtucket, Rhode Island) was computed to compare with the experimental results. A mesh was manually generated consisting of 10 mm, 8-node, solid cube linear elements. The cube's material properties (as measured in [Ott01]) are isotropic and linear with a Young's modulus of 15.3 kPa and an assumed Poisson's ratio of 0.499. Large deformation (i.e. nonlinear) analysis was employed using the boundary conditions and geometry extracted from the CT scans for the unloaded and 18.25% nominal strain cases.

3. Results

Figure 4 illustrates the processing of the data, beginning with segmented CT data for the *x-z* slice through the center of the cube, in both unloaded (Figure 4A) and 18.25% strain (Figure 4B) cases. Figure 4C shows the bead displacements throughout the cube combined for all four stain levels, while Figure 4D represents the displacement field for the central *x-z* slice. Reconstructions of the outer surface of the cube for each strain state is shown in Figure 4E. The estimated error of the bead locations is 2 mm.

The results from the FEM model are shown in Figure 5A, in the form of a plot for the *x-z* slice through the center of the cube with displacement magnitude coded as color. Figure 5B shows the FEM and experimental displacement vectors for each bead in this slice. The coordinates of a sample of 10 of the beads are presented in Table 1, together with their displacements from the FEM and experimental measurements, and the differences between these estimates. Full results are available on the project web site, http://biorobotics.harvard.edu/truthcube/.

4. Discussion

The results presented here demonstrate the potential of this technique for establishing physical standards for validating real time soft tissue simulations. The construction of the cube was straightforward and resulted in a structure with a modulus in the range of soft organs. Imaging under strains of over 18% was readily accomplished. The external surface and the fiducial beads were easily segmented, which permitted calculation of the displacement fields throughout the volume. The result is a displacement data set with well-characterized material properties and boundary conditions.

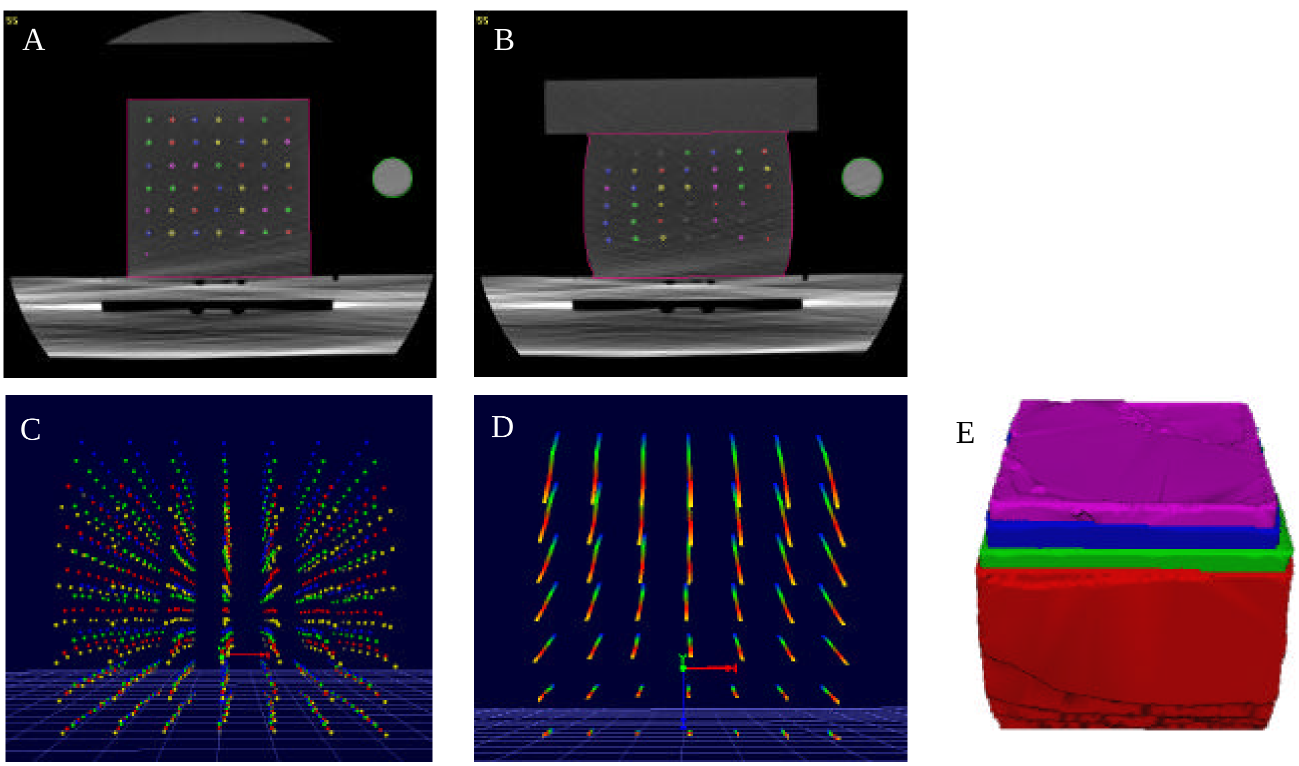

Figure 4: The CT image of the central *x-z* plane of the "Truth Cube" after segmentation in both the (A) unloaded and (B) maximally compressed states; the upper registration sphere is noticeable in these images. (C) 3_d perspective view of the centroids of best-fit spheres for all 343 beads in all strain states (blue = unloaded, green = 5%, red = 12.5 %, yellow = 18.25% strain). (D) Trajectory of the beads in the *x-z* central plane of (C). (E) Outer surfaces of the cube in its 4 strain states (purple = unloaded, red = 18.25%).

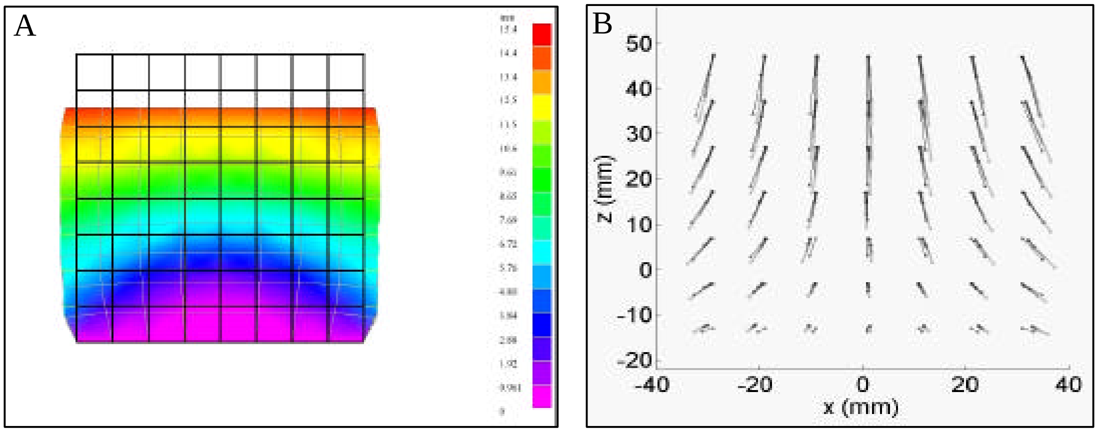

Figure 5: A comparison of the finite element displacement field and the CT experimental data displacement field for the central XZ plane. (A) A picture of the displacement of the uncompressed (black) and compressed (colored) mesh. (B) A comparison of the finite element results (thin black lines) and experimental results (grey-scale lines).

Bead initial location			Displacement (FEM)			Displacement (experimental)			|| Exp disp - FEM disp ||
X [mm]	Y [mm]	Z [mm]	dX [mm]	dY [mm]	dZ [mm]	dX [mm]	dY [mm]	dZ [mm]	[mm]
-29.0	3.0	-47.0	-3.3	0.0	12.9	-1.3	0.7	15.3	3.3
-19.0	3.0	-47.0	-2.3	0.0	12.7	0.0	0.7	15.2	3.5
-9.0	3.0	-47.0	-1.2	0.0	12.6	0.6	0.4	15.1	3.1
1.0	3.0	-47.0	0.0	0.0	12.6	1.3	0.4	15.1	2.8
11.0	3.0	-47.0	1.2	0.0	12.6	3.1	0.6	14.9	3.0
...	...	...	...	...	...	...	...	...	...
...	...	...	...	...	...	...	...	...	...
-9.0	3.0	13.0	-0.6	0.0	0.6	-0.6	0.4	1.2	0.7
1.0	3.0	13.0	0.0	0.0	0.7	0.1	0.2	1.1	0.4
11.0	3.0	13.0	0.6	0.0	0.6	0.7	0.2	1.3	0.7
21.0	3.0	13.0	1.3	0.0	0.8	1.8	0.1	1.2	0.6
31.0	3.0	13.0	2.1	0.0	0.6	3.0	0.0	1.8	1.5

Table 1: A representative set of 10 bead locations at rest and after 18.25% strain (14.6 mm compression) evaluated by both FEM and experimental data. The final column is the difference in bead location between the two evaluations.

These results are readily compared with the output of computational models. The simple FEM calculation presented here used a minimal number of elements to reflect some of the speed-vs-accuracy tradeoffs of real-time tissue simulations. The maximum differences with the experimental results were on the order of 3.5 mm for a displacement of about 15 mm. This is a relatively small difference, as might be expected for these simple geometric and loading conditions, and considering the estimated 2 mm accuracy of the measurement. Some portion of the difference may also be due to inexact specification of the boundary conditions on the top of the cube during compression. Nonetheless, refinement of the model (e.g. smaller mesh size) should bring closer agreement to the experiment. For more complex geometries, materials, and loading conditions, much larger differences can be expected between FEM results and reality, which this type of experimental data can help quantify.

Several refinements to the measurement techniques are indicated by these results. First, we have only estimated the accuracy of the bead positions in this initial dataset. More precise accuracy specifications can be obtained through an analysis of the imaging and image processing procedures, and through reproducibility measurements. The raw scan data will be available on the web site, so other users are also welcome to develop improved image processing algorithms for this purpose. Another area for better characterization is the top surface boundary condition, where oiling the cube served to limit and regularize friction, but where a “frictionless” condition clearly did not apply. Fortunately, the contact area is readily measured during the experiment and in the processed CT images, so additional boundary information is available.

4.1 Future Work

Our immediate plans are to complete tests of the truth cube, with a goal of improving the accuracy of the fiducial position estimation process and the boundary conditions. We will also develop additional loading capabilities, including indentation, shear, and torsion, to better reflect the range of surgical manipulations.

While this initial study demonstrated the feasibility of experimental measurement of volumetric displacement fields for soft materials under large strains, the truth cube itself is of limited value for validating soft tissue models. The cube has regular geometry and material properties that are helpful for the development process, but fast tissue simulations must deal with conditions that are vastly different, involving very large deformations, irregular shapes and complex materials. These are also the conditions where validation using traditional FEM techniques is most problematic.

The next phase of this project is thus the measurement of biological tissue volumetric displacements, in the form of an entire organ. Preliminary plans call for measurement of a porcine liver immediately post mortem. Fiducials will be inserted via needles throughout the parenchyma, followed by the imaging and image processing procedures reported here. In addition, a cast of the external shape of the liver will enable the creation of a silicone rubber model with bead fiducials where the material properties will be well-characterized. Simulation developers can then separately consider issues of large deformation and material complexities.

While these biological material tests have obvious advantages, the material properties will not be well-characterized as in the rubber tests. The identification of these material properties is an active area of research, and the data sets may be useful for solving the inverse problem of estimating these material properties from the displacement data. In any case, the data will provide a source of information for the development of fast simulation systems.

As we proceed, we welcome comments and suggestions on all aspects of the project, from tissue selection and loading conditions to experimental methods and data analysis. Further information is provided on the web site at: http://biorobotics.harvard.edu/truthcube. Contributions of a broad cross-section in the tissue modeling community will help ensure the development of a robust physical standard for the benchmarking of real-time soft tissue simulations.

4. Acknowledgements

This work was supported by U.S. Army Medical Research Acquisition Activity under contract DAMD17-01-1-0677. The Whitaker Foundation provided graduate student support.

6. References

[Ast98] Astley, O., Hayward, V. Multirate haptic simulation achieved by coupling finite element meshes through norton Equivalents. Proc. IEEE Int. Conf. on Robotics and Automation, 1998.

[Cot96] S. Cotin, H. Delingette, J.M. Clément, M. Bro-Nielsen, N. Ayache, J. Marescaux: *Geometrical and Physical Representations for a Simulator of Hepatic Surgery*, Proc. Medicine Meets Virtual Reality IV (MMVR'96), 1996, pp. 139-150.

[De01] S. De, J. Kim and M.A. Srinivasan. *Virtual surgery simulation using a collocation-based method of finite spheres*. First M.I.T. Conference on Computational Fluid and Solid Mechanics, 2001.

[Kuh97] Kühnapfel UG, Kuhn C, Hübner M, Krumm HG, MaaE H, Neisius B. *The Karlsruhe Endoscopic Surgery Trainer as an example for virtual reality in medical education*, Minimally Invasive Therapy and Allied Technologies, 1997:(6);122-125.

[Osm00] Osman, N.F.; McVeigh, E.R.; Prince, J.L. *Imaging heart motion using harmonic phase MRI*. IEEE Transactions on Medical Imaging vol.19, no.3 186-202 March 2000.

[Ott01] M. Ottensmeyer, *Minimally Invasive Instrument for In Vivo Measurement of Solid Organ Mechanical Impedance*, Doctoral Thesis in Mechanical Engineering at the Massachusetts Institute of Technology. © M.I.T., 2001.

[Pic01] G. Picinbono, H. Delingette, and N. Ayache. *Non-linear and anisotropic elastic soft tissue models for medical simulation*. In ICRA2001: IEEE International Conference Robotics and Automation, Seoul Korea, May 2001.

[Pip91] Pipe, J.G.; Boes, J.L.; Chenevert, T.L. Method for measuring three-dimensional motion with tagged MR imaging *Radiology*181: 591, 1991.

[Str98] N. Strumas, O. Antonyshyn, M.J. Yaffe, G. Mawdsley, and P. Cooper. *Computed Tomography Artifacts: an experimental investigation of causative factors*. Canadian Journal of Plastic Surgery, 1998; 6(1):23-29.

[Wel00] P.W. Wellman, R.D. Howe. *Breast tissue stiffness in compression is correlated to histological diagnosis*. Submitted to the Journal of Biomechanics. 2000.

[Wel99] P.W. Wellman. *Tactile imaging*. Ph.D. Thesis, Division of Engineering and Applied Sciences, Harvard University, 1999.

[Zha97] M. Zhang, Y.P. Zheng, and A.F.T. Mak. *Estimating the effective Young's modulus of soft tissues from indentation tests – nonlinear finite element analysis of effects of friction and large deformation*. Med. Eng. Phys. Vol. 19, No. 6 pp512-517, 1997.